

Dual-Band MIMO Antenna Array for Compact 5G Smartphones

Guobo Wei and Quanyuan Feng*

Abstract—An eight-port antenna system for fifth-generation (5G) multi-input multi-output (MIMO) mobile communication in smartphones is proposed, working in 3.5 GHz frequency band (3400–3600 MHz) and 5 GHz frequency band (4800–5100 MHz). The presented eight-port antenna array consists of four vertical structure antennas placed at four corners and four horizontal structure antennas etched along the two long sides of the circuit board. The height of vertical structure is only 4 mm, which is suitable for ultra-thin smartphones. The design of eight-port antenna array was fabricated and measured. According to the test results, an ideal impedance matching (superior to 10 dB), preeminent isolation (superior to 17 dB), and excellent efficiency (superior to 61%) are obtained over the 3.5 GHz frequency band and 5 GHz frequency band. In order to evaluate MIMO performance, the ergodic channel capacities and envelope correlation coefficients (ECC) are also investigated.

1. INTRODUCTION

For the past few years, there is a hot trend of multi-input multi-output (MIMO) antenna with the development of 5G communication, because MIMO technology can afford low co-channel interference, high data rate, and low loss of signal [1]. World Radio Communication Conference 2015 (WRC-15) allocated the 3.5 GHz band (3400–3600 MHz) to 5G mobile service bands in November 2015 [2]. In China, 3400–3600 MHz and 4800–5100 MHz are assigned for 5G mobile communication.

Several MIMO antennas have been presented for 5G mobile terminals [3–8]. A dual-band ten-port antenna array operating at long term evolution (LTE) 42/43/46 bands comes up with 10 T-shaped coupled fed slots [3]. However, antenna efficiencies of the system is not high. A hybrid antenna is created for 4G/5G MIMO mobile applications [6]. The 4G antenna module is a two-antenna array with a neutralization line to improve isolation, covering the GSM850/900/1800/1900, UMTS2100, and LTE2300/2500 operation bands. The 5G antenna module is an eight-port antenna array along the long edges, covering the 3.5 GHz band (3400–3600 MHz), and isolation is superior to 10 dB. Some integrated 4G/5G MIMO antenna arrays use the concept of connected antenna array (CAA) [9–11]. The multi-band antenna system uses two rectangular ring grooves around the ground plane to serve as radiating structures, eventually covering 1975–3540 MHz and 16.50–17.80 GHz. This designed structure is compact, planar, and easy to manufacture in [11]. With the popularity of full-screen mobile phone, side-edge frame antenna is a hot topic in current research [12–17]. A MIMO antenna array printed along the long frame of the phone is presented in [12], working in the 3.5 GHz band and 5 GHz band. Each antenna array consists of a gap-coupled branch and a curved monopole, fed by a 50 Ω microstrip line. In [15], similarly, a side-edge frame antenna array containing T-shaped feeding and U-shaped radiating elements is reported, working at the 3.5 GHz band (3400–3600 MHz). A multiband MIMO antenna array is designed for metal-rimmed mobile phone applications in [17], based on a 2-mm wide ring slot which is realized between the metal rim and ground. In order to reduce the coupling between multiple ports,

Received 30 December 2019, Accepted 22 January 2020, Scheduled 7 February 2020

* Corresponding author: Quanyuan Feng (fengquanyuan@163.com).

The authors are with the Institute of Microelectronics, University of Southwest Jiaotong, Chengdu, Sichuan, China.

neutralization technology is often used to improve isolation [18]. In addition, the appropriate defective structures can also reduce coupling and slightly contribute to impedance matching adjustment [19].

In this paper, an eight-port antenna array operating in the 3.5 GHz frequency band and 5 GHz frequency band for 5G smartphones is proposed. The proposed eight-port antenna design consists of four symmetric vertical structure elements and four symmetric horizontal structure elements, with small requirements for clearance area. The vertical structure is only 4 mm high, which is suitable for ultra-thin smartphones. The proposed eight-port mobile phone antenna array is simulated, fabricated, and measured. Typical parameters such as S -parameter, isolation, peak gain, and antenna efficiency are given in the article. In order to appraise the MIMO performance, the channel capacity and ECC are also shown.

2. DESIGN OF THE PROPOSED ANTENNA

The proposed dual-band MIMO antenna array is given in Fig. 1, which is composed of two similar antenna modules: vertical structure and horizontal structure. An FR4 substrate (relative permittivity = 4.4, loss tangent = 0.02) is selected as system circuit board with a representative dimension of 150 mm \times 70 mm \times 0.8 mm, which is suitable for a 5.5-inch smartphone. Each antenna element is composed of a 50 Ω L-shaped feeding line and a complex rectangle-shaped slot. In Fig. 1(a), the main view of the proposed antenna array is exhibited. The details of the vertical (Ant 1–4) and horizontal structures (Ant 5–8) are indicated in Figs. 1(b) and (c). The high isolation of Ant 1 and Ant 5 is mainly realized by using orthogonal (vertical and horizontal) arrangement. Because the eight antenna elements are similar, the following discussion results are general, and the horizontal antenna unit is selected for discussion.

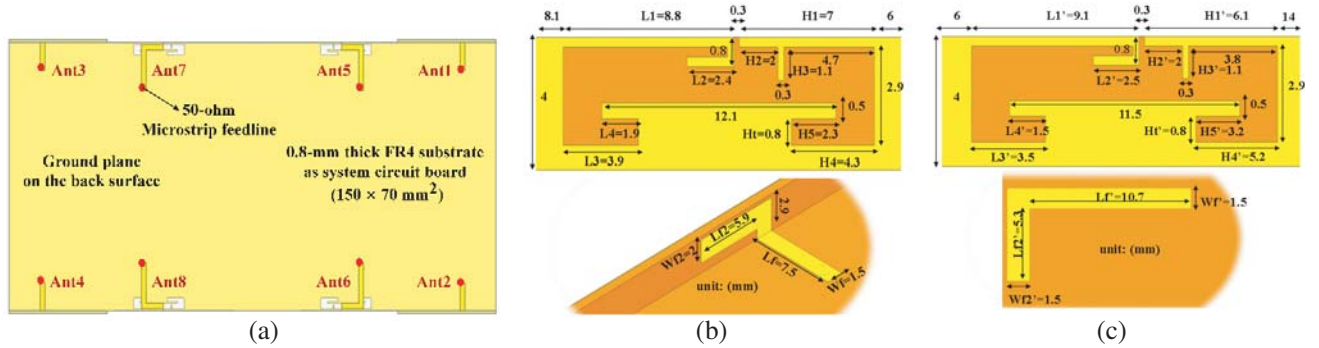


Figure 1. Detailed dimensions of the designed MIMO antenna. (a) Overall structure. (b) Vertical structure. (c) Horizontal structure.

The detailed structure of the antenna unit is described in Fig. 1(b). A compact rectangle-shaped slot is etched on the ground with a size of 16.8 mm \times 2.9 mm, serving as a radiator. The rectangular slot is divided into two parts by digging out a square section (0.3 mm \times 0.3 mm), and a T-shaped prominent structure is attached to adjust impedance matching. The lengths of AA' sections are nearly quarter-wavelength, which is shown in Fig. 2. In Fig. 2(a), the surface current distribution of the proposed antenna at 3.5 GHz is shown, and along the AA' branch a quarter-wavelength (\approx 22 mm) surface current distribution is observed. Analogically, a quarter-wavelength (\approx 15 mm) surface current distribution is observed along the BB' section in Fig. 2(b). Therefore, dual bands of 3.5 GHz and 5 GHz can be obtained by suitable adjustment of AA' and BB'. In order to determine accurate parameters, the parameters of AA' and BB' are swept and analyzed. In Fig. 3(a), the length of L1' can control the low frequency resonance, and the high frequency is hardly affected. L2' is a curved branch of the AA' section in order to appropriately reduce antenna size, and also affects low frequency resonance in Fig. 3(b). In the design process, L1' is used for coarse tuning and L2' used for sensitive adjustment, and the final optimal values are 9.1 mm and 2.5 mm. Similarly, H1 and H3 as parts of the BB' section can decide the high frequency resonance. In Fig. 4, the optimal lengths of H1' and H3' are 6.1 mm and

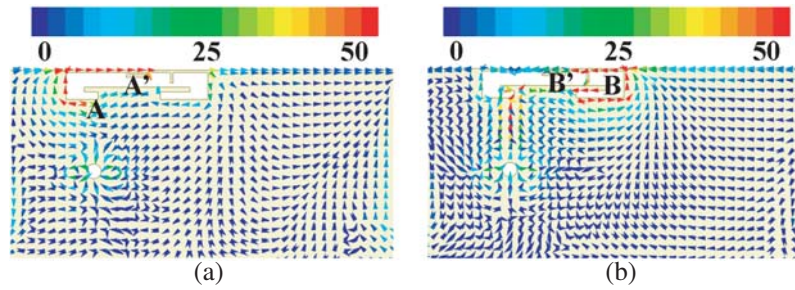


Figure 2. Simulated current distributions of the designed antenna at (a) 3.5 GHz and (b) 5 GHz.

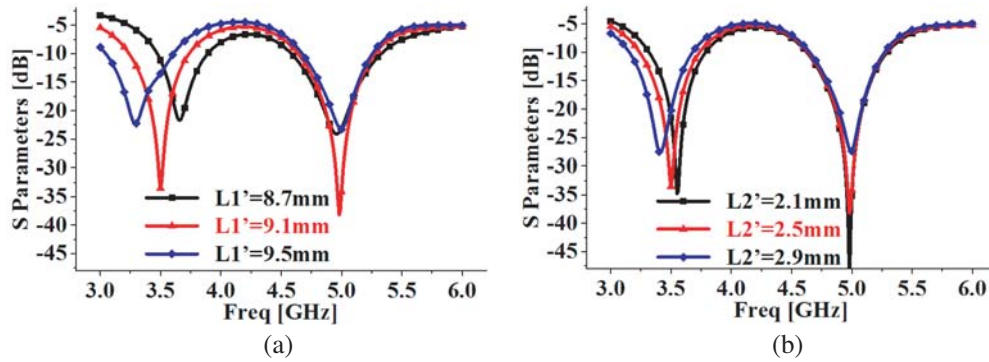


Figure 3. Reflection coefficients for varying length of (a) $L1'$ and (b) $L2'$.

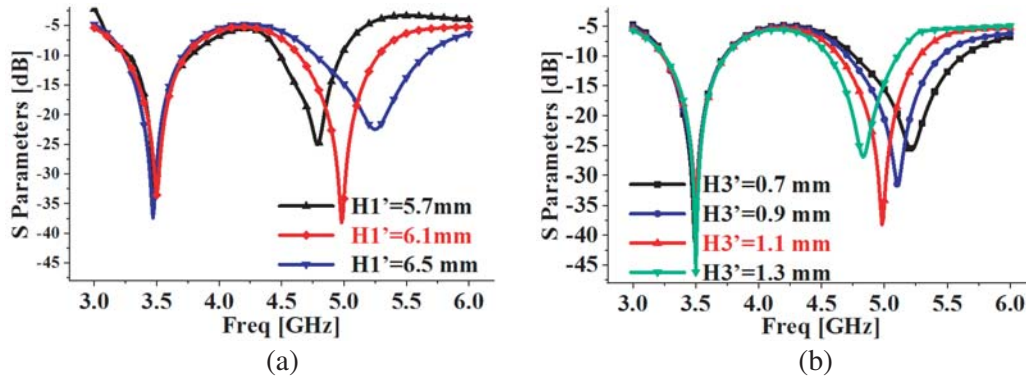


Figure 4. Reflection coefficients for varying length of (a) $H1'$ and (b) $H3'$.

1.1 mm, making the antenna operating band at 5 GHz.

Each antenna element has a prominent T-shaped structure in the gap of the ground plane to obtain the optimized impedance matching. Fig. 5(a) shows that adjusting the height of the T-shaped structure can effectively tune the impedance matching. When the height is 0.8 mm, the impedance matching of dual band is optimal. The designed antenna unit is fed by an L-shaped microstrip line, and the size of line is related to impedance matching. With tuning the length of line, the ideal impedance matching of operating band is obtained at $Lf2' = 6.8$ mm in Fig. 5(b).

Eight antenna elements are arranged into an antenna array as shown in Fig. 1, and parameters of each unit have been fine-tuned as analyzed above. The best result is shown in Fig. 6. Only S_{11} (vertical substrate) and S_{55} (horizontal substrate) are given because antenna structures are similar and symmetrical. Ant 1 and Ant 5 have exhibited 10 dB (2 : 1 VSWR) impedance bandwidths over the low frequency band (3400–3600 MHz) and high frequency band (4800–5100 MHz).

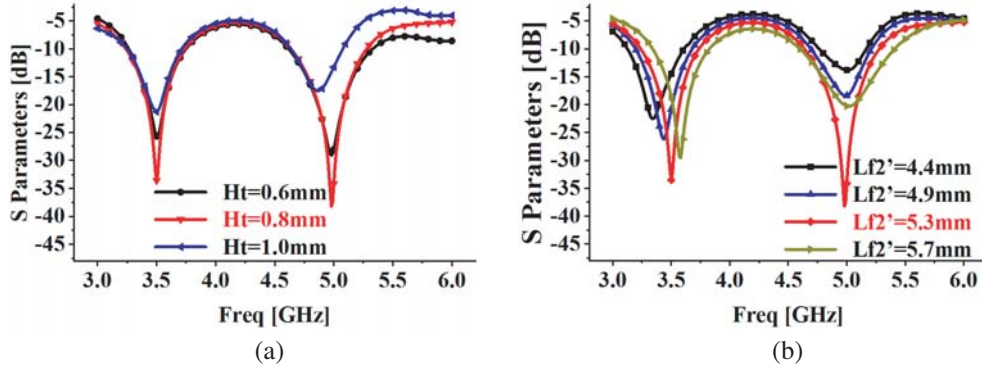


Figure 5. Impedance matching of varying (a) Ht' and (b) $Lf2'$.

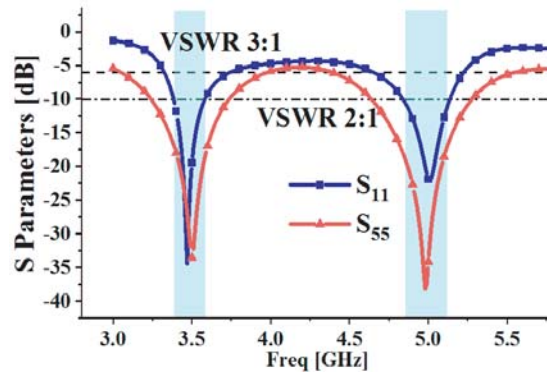


Figure 6. Simulated reflection coefficients of Ant 1 and Ant 5.

3. RESULTS AND DISCUSSION

A prototype of the eight-port MIMO antenna array is manufactured and measured to validate the simulation results. As demonstrated in Fig. 7, each antenna element is directly connected to a $50\ \Omega$ coaxial sub-miniature A (SMA) connector. The reflection coefficients of designed antenna are measured by an Agilent E5071C vector network analyzer.

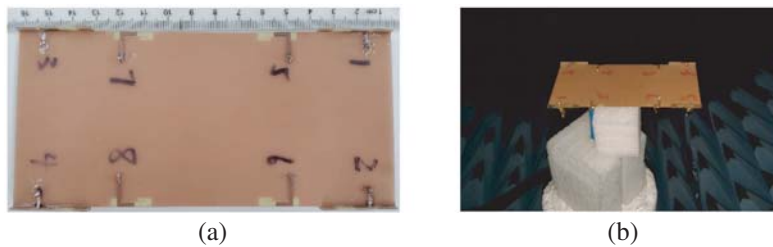


Figure 7. Pictures of (a) the manufactured prototype. (b) Test-site.

3.1. S-Parameters

The measured and simulated results of S -parameters for Ant 1 to Ant 8 are compared in Fig. 8. In Fig. 8(a), the maximum bandwidths (10 dB) of measurement in the low frequency band and high frequency band are 3400–3650 MHz and 4650–5220 MHz by Ant 3. The maximum bandwidths (10 dB) are 3280 MHz–3780 MHz and 4620–5520 MHz by Ant 7 in Fig. 8(b). The bandwidths of the vertical

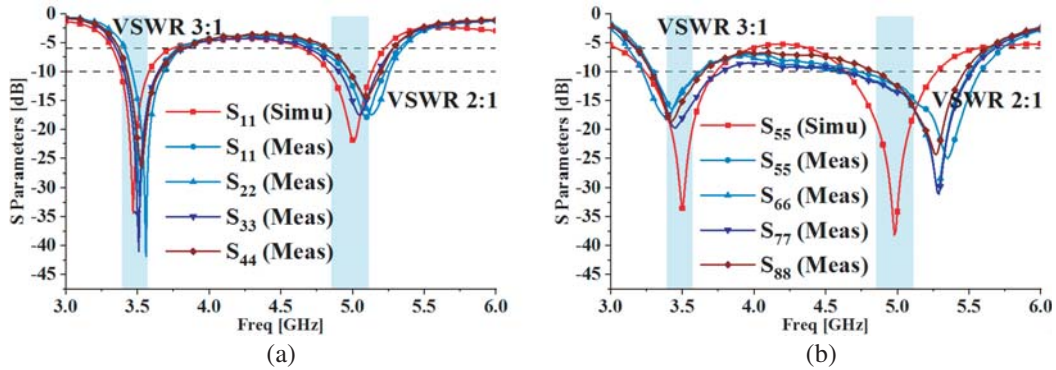


Figure 8. Measured and simulated results of S -parameters. (a) Ant 1 to Ant 4. (b) Ant 5 to Ant 8.

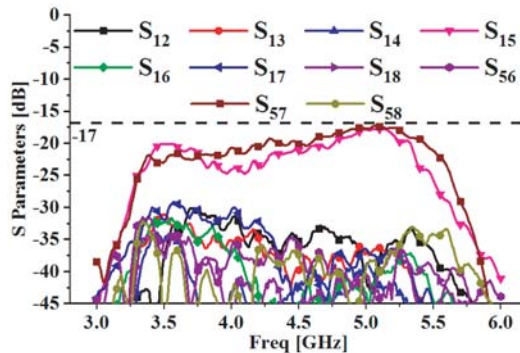


Figure 9. Measured isolations of proposed MIMO antenna array.

structure are slightly less than that of the horizontal structure, but it also meets the optional band. This structure arrangement can effectively improve the isolation.

Therefore, the vertical structure (Ant 1 to Ant 4) and horizontal structure (Ant 5 to Ant 8) have good 10 dB impedance bandwidths, covering the 3.5 GHz band (3400–3600 MHz) and 5 GHz band (4800–5100 MHz). Moreover, the isolations of Ant 1 vs Ant 5 and Ant 5 vs Ant 7 are superior to 17 dB with the structure arrangement, while others are all better than 30 dB, and only partial results are shown in Fig. 9 due to symmetry and similarity.

3.2. Antenna Efficiencies and Radiation Patterns

With one port excited and others loaded with 50-ohm loads, the antenna efficiencies and gains can be obtained, and the measured results are given in Fig. 10. It is obvious that antenna efficiencies vary from 61% to 74% over the operating band in Fig. 10(a), while antenna gains are approximately 3.4–4.4 dB and 5–5.5 dB over the desired frequency bands in Fig. 10(b).

The radiation patterns of the designed antenna array at 3.5 GHz and 5 GHz are measured and shown in Figs. 11–12. Because of the symmetry of the designed MIMO antenna system, only measured results of Ant 1 and Ant 5 are exhibited. The Gain-phi and Gain-theta manifest good complementary characteristic. In the main lobe directions, the co-polarization is at least at 10–19 dB (for Ant 1 and Ant 5) larger than its corresponding cross-polarization. Therefore, the proposed MIMO antenna array system can obtain a good pattern and polarization diversity.

3.3. MIMO Performance

In addition to reflection coefficient, isolation, antenna efficiency, and radiation pattern, ECC is an effective parameter to estimate the characteristic of MIMO antenna array, and the optimized value should be usually less than 0.5. The ECC can be computed using the formula based on the measured

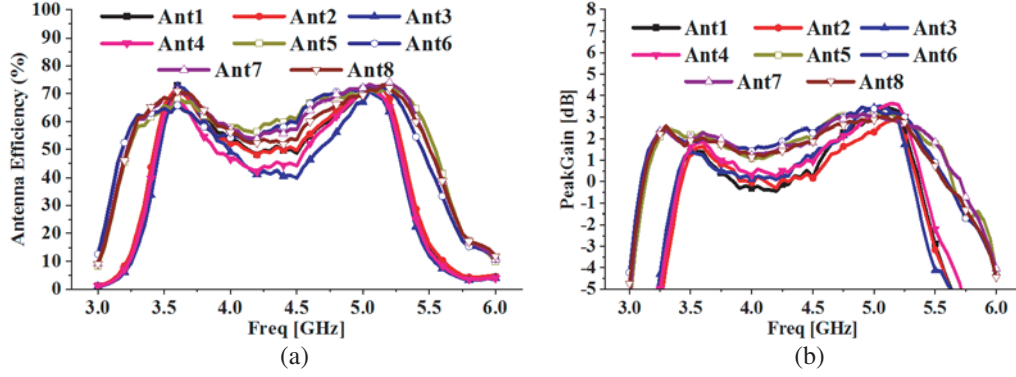


Figure 10. Measured results of designed antenna. (a) Efficiencies. (b) Gains.

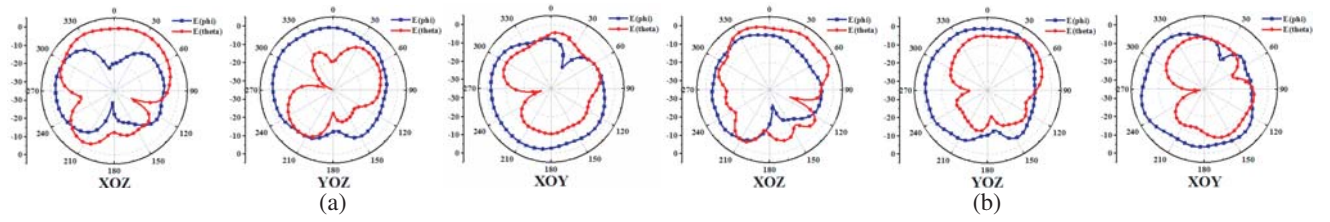


Figure 11. Measured radiation patterns of Ant 1 at three principal planes. (a) at 3.5 GHz and (b) 5 GHz.

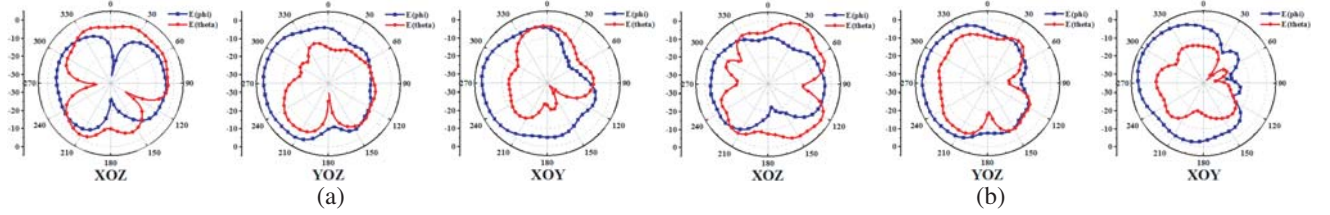


Figure 12. Measured radiation patterns of Ant 5 at three principal planes. (a) at 3.5 GHz and (b) 5 GHz.

Fairfield results [20], and $\vec{F}_i(\theta, \varphi)$ is the three-dimensional field radiation pattern. According to the measured results, the values of ECC are calculated in Fig. 13, and the calculated ECCs are better than 0.01 over the operating bands.

$$p_{eij} = \frac{\left| \iint_{4\pi} \left[\vec{F}_1(\theta, \varphi) * \vec{F}_2(\theta, \varphi) \right] d\Omega \right|^2}{\iint_{4\pi} \left| \vec{F}_1(\theta, \varphi) \right|^2 d\Omega \iint_{4\pi} \left| \vec{F}_2(\theta, \varphi) \right|^2 d\Omega} \quad (1)$$

Therefore, the prototype of the proposed eight-port antenna array shows excellent spatial diversity characteristics. Compared to a single input single output (SISO) antenna system, MIMO antenna system greatly improves channel capacity to satisfy 5G communication. Assume that each transmit antenna is allocated equal power, and channel capacity can be calculated [20].

$$C = \log_2 \left[\det \left(I_N + \frac{\rho}{N} H H^T \right) \right] \quad (2)$$

where ρ is the average signal to noise ratio (SNR), N the number of elements, H the normalized covariance channel matrix, and I_N an $N \times N$ identity matrix. The ergodic channel capacity can be

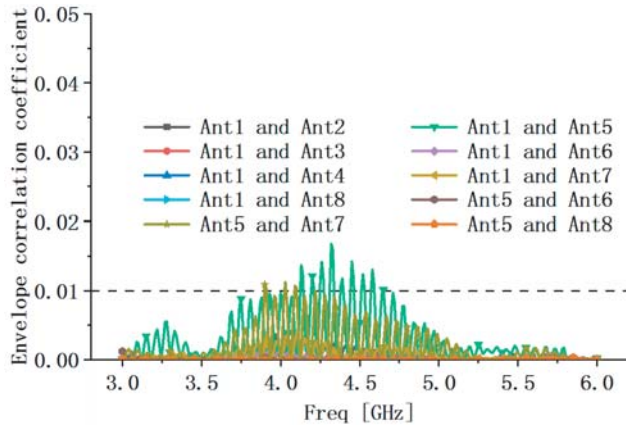


Figure 13. Calculated ECC values.

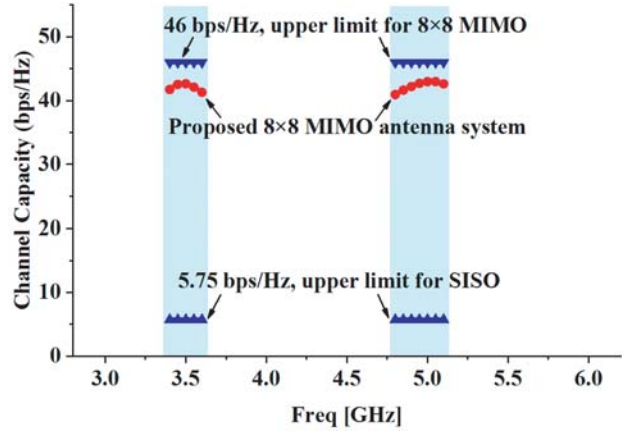


Figure 14. Calculated ergodic channel capacities.

calculated by using an independent and identically distributed Rayleigh fading channel (20 dB SNR). As shown in Fig. 14, the maximum computed values of the ergodic channel capacities are approximately 42.6 and 43 bps/Hz over low frequency band (LB) and high frequency band (HB), almost 7.5 times the ideal channel capacity of a SISO system (5.75 bps/Hz) and approach the ideal value (46 bps/Hz). Obviously, the proposed 8-element MIMO antenna exhibits excellent spatial multiplexing capability. Table 1 exhibits the comparison of the designed antenna array with the previous reference. Compared to the references, the proposed antenna system shows better impedance matching bandwidth, low isolation, high antenna efficiency, and excellent MIMO performance at the operating bands.

Table 1. Comparison of the referenced and proposed antenna.

Reference	Bandwidth (GHz)	Isolation (dB)	Efficiency (%)	Channel Capacity (bps/Hz)
3	3.4–3.8 (LB) 5.1–5.9 (HB) (–6 dB)	> 11	42–65 (LB) 62–82 (HB)	16.2×3
4	3.4–3.8 (–6 dB)	> 10	40–62	8×3
5	3.4–3.8 (–6 dB)	> 12	30–53	8×3
6	3.4–3.6 (–10 dB)	> 10	62–78	16.7×3
12	3.4–3.6 (LB) 4.8–5.1 (HB) (–6 dB)	> 11.5	41–72 (LB) 40–85 (HB)	15×7
15	3.4–3.6 (–10 dB)	> 20	60–70	17.4×6
Proposed Antenna	3.4–3.6 (LB) 4.8–5.1 (HB) (–10 dB)	> 17	61–72 (LB) 64–74 (HB)	15.2×2.9

4. CONCLUSION

A compact dual-band MIMO antenna array for 5G mobile terminals is put forward in this article. The designed antenna is easy to adjust, small in size, and fabricated on a $150 \times 70 \times 0.8 \text{ mm}^3$ FR4 substrate. The reflection coefficient and transmission coefficient are superior to 10 dB and 17 dB, respectively. Acceptable radiation efficiencies (better than 61%), high gains (better than 3.4 dB), and preeminent ECC values (less than 0.01) over the whole bandwidths are achieved. Furthermore, the peak channel capacities of the fabricated 8×8 MIMO antenna array are 42.6 and 43 bps/Hz in LB and HB, which are nearly 7.5 times of a traditional SISO system. Therefore, the designed antenna system exhibits excellent radiation and superior MIMO performance, and is an eligible candidate for 5G smartphone applications.

ACKNOWLEDGMENT

This work is supported by Key Project of the National Natural Science Foundation of China under Grant 61531016, 61831017 and the Sichuan Provincial Science and Technology Important Projects under Grant 19ZDYF29042018ZDZX0148 and 2018GZDZX0001.

REFERENCES

1. Andrews, J. G., et al., "What will 5G be?" *IEEE J. Sel. Areas Commun.*, Vol. 32, No. 6, 1065–1082, Jun. 2014.
2. WRC-15 Press Release, (Nov. 27, 2015), World Radiocommunication Conference Allocates Spectrum for Future Innovation, [Online], Available: http://www.itu.int/net/pressoffice/press_releases/2015/56.aspx.
3. Li, Y.-X., C.-Y.-D. Sim, Y. Luo, and G.-L. Yang, "Multiband 10-antenna array for sub-6 GHz MIMO applications in 5-G smartphones," *IEEE Access.*, Vol. 6, 28041–28053, May 2018.
4. Wong, K.-L. and J. Y. Lu, "3.6-GHz 10-antenna array for MIMO operation in the smartphone," *Microw. Opt. Technol. Lett.*, Vol. 57, No. 7, 1699–1704, Jul. 2015.
5. Wong, K.-L., J.-Y. Lu, L.-Y. Chen, W.-Y. Li, and Y.-L. Ban, "8-antenna and 16-antenna arrays using the quad-antenna linear array as a building block for the 3.5-GHz LTE MIMO operation in the smartphone," *Microw. Opt. Technol. Lett.*, Vol. 58, No. 1, 174–181, Jan. 2016.
6. Ban, Y.-L., C. Li, and C.-Y.-D. Sim, "4G/5G multiple antennas for future multi-mode smartphone applications," *IEEE Access.*, Vol. 4, 2981–2988, Jun. 2016.
7. Qin, Z., W. Geyi, M. Zhang, and J. Wang, "Printed eight-element MIMO system for compact and thin 5G mobile handset," *Electron. Lett.*, Vol. 52, No. 6, 416–418, 2016.
8. Ban, Y.-L., C. Li, C.-Y.-D. Sim, G. Wu, and K.-L. Wong, "4G/5G multiple antennas for future multi-mode smartphone applications," *IEEE Access.*, Vol. 4, 2981–2988, 2016.
9. Neto, A., D. Cavallo, G. Gerini, and G. Toso, "Scanning performances of wide band connected arrays in the presence of a backing reflector," *IEEE Trans. Antenna Propag.*, Vol. 57, No. 10, 3092–3102, Oct. 2009.
10. Cavallo, D., A. Neto, G. Gerini, A. Micco, and V. Galdi, "A 3 to 5 GHz wideband array of connected dipoles with low cross polarization and wide-scan capability," *IEEE Trans. Antennas Propag.*, Vol. 61, No. 3, 1148–1154, Mar. 2013.
11. Sharawi, M. S., M. Ikram, and A. Shamim, "A two concentric slot loop based connected array mimo antenna system for 4G/5G terminals," *IEEE Trans. Antennas Propag.*, Vol. 65, No. 12, 6679–6686, Dec. 2017.
12. Guo, J.-L., L. Cui, C. Li, and B.-H. Sun, "Side-edge frame printed eight-port dual-band antenna array for 5G smartphone applications," *IEEE Trans. Antennas Propag.*, Vol. 66, No. 12, 7412–7417, Dec. 2018.
13. Wong, K.-L. and C.-Y. Tsai, "Half-loop frame antenna for the LTE metalcasing tablet device," *IEEE Trans. Antennas Propag.*, Vol. 65, No. 1, 71–81, Jan. 2017.

14. Yuan, B., Y. Cao, G. Wang, and B. Cui, "Slot antenna for metal-rimmed mobile handsets," *IEEE Antennas Wireless Propag. Lett.*, Vol. 11, 1334–1337, Nov. 2012.
15. Zhao, A.-P. and Z.-Y. Ren, "Size reduction of self-isolated MIMO antenna system for 5G mobile phone applications," *IEEE Trans. Antennas Propag. Lett.*, Vol. 18, No. 1, 152–156, Nov. 2018.
16. Aziz, R. S., A. K. Arya, and S.-O. Park, "Multiband full-metal-rimmed antenna design for smartphones," *IEEE Antennas Wireless Propag. Lett.*, Vol. 15, 1987–1990, Mar. 2016.
17. Chen, Q.-G., J.-P. Wang, L. Ge, Y.-J. Li, T.-Q. Pei, and C.-Y.-D. Sim, "Single ring slot based antennas for metal-rimmed 4G/5G smartphones," *IEEE Trans. Antennas Propag.*, Vol. 67, No. 3, 1476–1478, Mar. 2019.
18. Wang, S., S. Member, and Z. Du, "Decoupled dual-antenna system using crossed neutralization lines for LTE/WWAN smartphone applications," *IEEE Antennas Wireless Propag. Lett.*, Vol. 14, 523–526, Nov. 2015.
19. Yang, Y., Q. Chu, and C. Mao, "Multiband MIMO antenna for GSM, DCS, and LTE indoor applications," *IEEE Trans. Antennas Propag. Lett.*, Vol. 15, 1573–1576, Jan. 2013.
20. Sharawi, M. S., "Printed multi-band MIMO antenna systems and their performance metrics," *IEEE Antennas and Propag. Magazine*, Vol. 55, No. 5, 218–232, Oct. 2013.